Supporting Information

Mishra et al. 10.1073/pnas.1422759112

SI Results

Genotype and Allele Distribution. The three groups were in Hardy–Weinberg equilibrium for the studied SNPs. Of 10 genotyped polymorphisms of *apelin*, rs3761581T/G, rs2235312T/C, and rs3115757G/C differed significantly between HAPE-p and HAPE-f ($P \leq$ 3.2E-03) (Table S3). Multivariate-logistic regression (MLR) analysis revealed significant higher risk of HAPE with alleles rs3761581G, rs2235312T, and rs3115757G, the adjusted risk-odds being above 2.5 and, hence, were recognized as risk alleles, whereas the alleles rs3761581T, rs2235312C, and rs3115757C that were overrepresented in healthy controls, HAPE-f, and HLs were recognized as protective alleles (P = 2.7E-03, 1.0E-06, and 3.2E-03, respectively). Of seven genotyped polymorphisms of *APLNR*, SNPs rs11544374G/A and rs2282623G/A differed significantly between HAPE-p and HAPE-f ($P \leq$ 0.011) (Table S4). MLR analysis revealed significant higher risk of HAPE for homozygotes rs11544374AA and rs2282623GG, the adjusted risk-odds being above 1.5 for these genotypes; as a consequence, the respective alleles were overrepresented in HAPE-p and were thus recognized as risk alleles, whereas the alleles rs11544374G and rs2282623A that were overrepresented in healthy controls were recognized as protective alleles (P = 0.004 and 0.013, respectively). Of 11 genotyped polymorphisms of *NOS3*, 4b/4a, rs1799983G/T, and rs7830A/C differed significantly between HAPE-p and HAPE-f ($P \leq$ 0.016) (Table S5). MLR analysis revealed significant higher risk of HAPE for homozygotes 4aa, rs1799983TT, and rs7830CC, the adjusted risk-odds being above 1.3 for these genotypes; as a consequence, the respective alleles were overrepresented in HAPE-p and were recognized as risk alleles, whereas the alleles 4b, rs1799983G, and rs7830A that were overrepresented in healthy controls were recognized as protective alleles (P = 3.0E-04, 0.037 and 1.6E-05, respectively).

Within-Gene Interactions. Maximum-likelihood analysis by Phase provided four haplotypes each of *apelin*, *APLNR*, and *NOS3*, which differed significantly between the groups ($P < 0.05$) (Table S6). These haplotypes exceeded the cut-off frequency of >2%. Of four, two haplotypes of *apelin*, G-T-G and T-T-G, were prevalent in HAPE-p compared with HAPE-f with odds ratios (ORs) of 16.22 and 1.50 (P = 4.0E-06 and 0.036, respectively) and with ORs of 7.42 and 2.04 compared with HLs (P = 0.015 and 4.6E-04, respectively), and hence were recognized as risk haplotypes. Similarly, the other two haplotypes of *apelin*, T-C-G and T-C-C, were prevalent in HAPE-f and HLs (P = 1.6E-04 and 1.0E-06, respectively) and were thus recognized as protective haplotypes. Of four *APLNR* haplotypes, only one haplotype, A-G, was prevalent in HAPE-p with an OR of 1.87 compared with HAPE-f (P = 0.0028) and with an OR of 1.63 compared with HLs (P = 0.02) and, hence, was recognized as risk haplotype. Similarly, haplotype G-A was prevalent in HAPE-f and HLs compared with HAPE-p with ORs of 0.66 and 0.27 (P = 0.03 and 0.001, respectively) and was therefore recognized as protective haplotype. Of four *NOS3* haplotypes, only one haplotype a-G-C was prevalent in HAPE-p with OR of 1.97 compared with HAPE-f (P = 0.013), and was thus recognized as risk haplotype, whereas two haplotypes, b-G-A and b-T-A were prevalent in HAPE-f and thus were recognized as protective haplotypes with ORs of 0.43 and 0.7 (P = 0.022 and 0.019, respectively).

Gene–Gene Interactions. The MDR model evaluated between-genes interactions. A four-locus model comprising of *apelin* rs3761581T/G, rs2235312T/C and *APLNR* rs11544374G/A, rs2282623G/A showed the interactions between apelin and *APLNR* (Fig. S1 *A*, *i*). Similarly, a two-locus model comprising of *apelin* rs2235312T/C and *NOS3* rs7830A/C showed the interactions between *apelin* and *NOS3* (Fig. S1 *A*, *ii*). The interactions between *apelin* rs3761581, rs2235312, and *APLNR* rs11544374, rs2282623 by MDR model (cross-validation consistency = 10/10) depicted the four-locus interaction rs3761581T/G-rs2235312T/C-rs11544374G/A-rs2282623G/A as the best disease-predicting model with testing balance accuracy of 0.68 (P = 0.028) in HAPE-p versus HAPE-f (Fig. S1 *A*, *i*). The GG-TT-GG-AG interaction was categorized as risk (P = 0.039), whereas TT-CC-AG-AG and TT-CC-GG-AG interactions were seen as protective (P = 0.028 and 0.024, respectively). A two-locus model between *apelin* rs3761581T/G and *APLNR* rs2282623G/A came as the best model in HAPE-p versus HLs with testing balance accuracy of 0.7603 (P = 1.2E-03) (Fig. S1 *B*, *i*). The GG-AG, TT-GG, and GG-GG interactions were categorized as risk ($P \leq$ 0.011), whereas TT-AA and TT-AG interactions were categorized as protective (P = 2.0E-06 and 1.0E-06, respectively). A two-locus model comprising of *apelin* rs2235312T/C and *NOS3* rs7830A/C emerged as the best disease-predicting model in HAPE-p vs. HAPE-f (Fig. S1 *A*, *ii*). The interacted genotype TT-CA and TT-CC were categorized as risk (P = 0.022 and 4.0E-04, respectively), whereas CC-AA and CC-CC were categorized as protective (P = 1.2E-05 and 0.022, respectively). Although in HAPE-p vs. HLs, a three-locus model comprising of *apelin* rs2235312T/C and *NOS3* rs7830A/C and 4b/4a emerged as the best disease-predicting model (Fig. S1 *B*, *ii*). The interacted genotypes TT-CA-ab, TT-CC-ab, and TT-CC-bb were categorized as risk ($P \leq$ 0.011), and CC-AA-bb and CC-CA-bb were categorized as protective (P = 1.8E-05 and 1.0E-05, respectively).

Causal Role of the Associated SNPs.

Contribution of risk alleles and haplotypes to apelin-13 level. A regression coefficient showed association of the *apelin* risk allele rs3761581G with decreased apelin-13 level in the three groups, HAPE-p, HAPE-f, and HLs ($P \leq$ 0.036) (Table 1, *Results*, and Fig. S3*A*). The *apelin* risk allele rs2235312T associated with a decreased apelin-13 level in HAPE-p and HLs only (P = 0.004 and 0.003, respectively) (Table 1 and Fig. S3*B*). Notably, rs3761581G associated with a decrease of 43.6%, 28.0%, and 43.7% in apelin-13 levels and rs2235312T associated with a decrease of 37.7%, 16.2%, and 25.9% in the levels in HAPE-p, HAPE-f, and HLs, respectively (Fig. S3 *A* and *B*). The *APLNR* risk allele rs11544374A associated with a decreased apelin-13 level in HAPE-p and HLs (P = 0.030 and 0.048, respectively). The *apelin* risk haplotypes G-T-G and T-T-G showed significant association with a decreased level in HAPE-p (P = 0.015 and 0.021, respectively). Understandably, the protective haplotype T-C-C was positively and significantly associated with the apelin-13 level in HAPE-p (P = 0.001). Another protective haplotype T-C-G was positively associated in HAPE-f and HLs (P = 0.039 and 0.002, respectively). The *APLNR* risk haplotype A-G associated inversely with the apelin-13 level in HAPE-p and HLs (P = 0.002 and 0.036, respectively) and the protective haplotype G-A associated positively with the apelin-13 level in HAPE-p (P = 0.008) (Table 1). *NOS3* risk alleles and haplotypes did not show associations with apelin-13 levels.

Contribution of risk alleles major haplotypes to nitrite level. Regression coefficients showed association of the *apelin* risk allele rs3761581G with decreased nitrite level in the three groups ($P \leq$ 0.044, respectively) (Table 2 and Fig. S3*C*). Another risk allele rs2235312T also associated with a decreased nitrite level in HAPE-p and HLs (P = 6.0E-04) (Table 2 and Fig. S3*D*). Notably, the rs3761581G

associated with a decrease of 20.7%, 29.6%, and 44.0% in nitrite levels and rs2235312T associated with a decrease of 32.9%, 14.3%, and 34.6% in the levels in HAPE-p, HAPE-f, and HLs, respectively (Fig. S3 *C* and *D*). Similarly, the *NOS3* risk alleles 4a, rs1799983T, and rs7830C associated with decreased nitrite level in HAPE-p and HLs ($P \leq 0.042$). The association of haplotypes of *apelin* and *NOS3* with nitrite level was equally noteworthy (Table 2). The *apelin*-susceptible haplotype G-T-G and T-T-G associated with a decreased nitrite level in HAPE-p ($P = 0.001$). The *apelin* protective haplotype T-C-C associated with an increased nitrite level in HAPE-p, HAPE-f, and HLs ($P \leq 0.05$). The other *apelin* protective haplotype T-C-G associated with an increased nitrite level in HAPE-p and HAPE-f (P = 8.2E-05 and 3.4E-06, respectively). In the case of *NOS3* haplotypes, the risk haplotype a-G-C associated with a decreased nitrite level ($P \leq 0.002$) and the protective haplotype b-G-A associated with increased nitrite level in the three groups, HAPE-p, HAPE-f, and HLs ($P \leq 0.027$). *APLNR* risk alleles and haplotypes did not show any such associations with nitrite levels.

Association of allelic interactions of apelin rs3761581 and rs2235312 with apelin-13 and nitrite levels. Here we looked for the influence of the two alleles together on the two biomarker levels. We analyzed the association of risk allele interaction (i.e., rs3761581G+rs2235312T) with apelin-13 and nitrite levels in comparison with the protective allele interaction rs3761581T+rs2235312C (Fig. S3 *E* and *F*). Notably, the interactions of these alleles more amply demonstrated the additional decrease in the levels of apelin-13 by 5.7%, 18.8%, and 5.1% than the individual allele rs3761581G and by 11.6%, 30.6%, and 22.9% than the allele rs2235312T in HAPE-p, HAPE-f, and HLs, respectively (Fig. S3*E*). Similarly, this interaction contributed more to an additional decrease in the levels of nitrite by 15.3%, 9.4%, and 9.2% than the allele rs3761581G and by 3.1%, 24.7%, and 18.6% than the allele rs2235312T in HAPE-p, HAPE-f and HLs, respectively (Fig. S3*F*).

SI Materials and Methods

Study Subjects. In a cross-sectional study, the subjects were categorized into three well-defined groups: (*i*) HAPE-patients (HAPE-p) were sojourners, who suffered the disorder upon exposure to HA (3500 m); (*ii*) HAPE-free sojourners (HAPE-f) were the healthy subjects, who visited HA under similar conditions and carried out routine strenuous physical activities but did not suffer from the disorder; and (*iii*) HLs. HAPE-p and HAPE-f were permanent residents of low altitude (<200 m) of north India and were of Indo-Aryan ethnicity. They traveled to altitudes (3,500–5,600 m) for various reasons, such as professional assignments, recreation, and adventure; HLs were permanent residents of altitude at and above 3,500 m for many generations with Tibeto-Burman ethnicity. Approximately 200 subjects in each group were recruited through Sonam Norboo Memorial (SNM) hospital, Leh (3,500 m), Ladakh, Jammu, and Kashmir, India.

Age, height, weight, body mass index (BMI), and clinical characteristics, such as blood pressure (BP), arterial oxygen saturation (SaO_2), and pulse rate were recorded in the three groups immediately upon admission. The subjects were given rest before BP measurement. Three measurements of BP, in supine position, using a calibrated mercury sphygmomanometer with appropriate adult cuff size were recorded; SaO_2 level was measured by Finger-Pulse Oximeter 503 (Criticare Systems). Before participation in the study, informed and written consent was obtained from each participant. The two human ethical committees, namely the human ethical committee of Council of Scientific and Industrial Research-Institute of Genomics and Integrative Biology, Delhi and the human ethical committee of SNM Hospital, Leh, had approved the investigation.

Selection Criterion of HAPE. HAPE is a noncardiogenic pulmonary edema that develops in otherwise healthy individuals upon rapid ascent to altitudes above 2,500 m. The symptoms develop gradually within the first 2–4 d at high altitude. Several clinical parameters were recorded to diagnose HAPE. The clinical symptoms included hypoxemia, cough, and dyspnea at rest, presence of pulmonary rales and cyanosis, below normal level SaO_2, and absence of infection. Chest radiography revealed infiltrates consistent with pulmonary edema. PASP was measured by Hewlett-Packard HP-Sonos 5500 echocardiography (ECG) machine in left lateral decubitus position with a 20° upper body tilt without prior O_2 inhalation. PASP was measured applying simplified Bernoulli formula using maximum velocity of tricuspid regurgitation peak flow added to a fixed value of 10 mmHg attributed as right atrial pressure. ECG was performed in the subjects of the three groups. Those patients who had poor window and in whom tricuspid regurgitation could not be recorded with satisfaction were excluded. Patients were subjected to ECG within 1–3 h of admission without prior O_2 inhalation.

PASP measurement was also used to exclude valvular disease and other associated cardiac anomalies. It also helped in differentiating pulmonary arterial diseases like primary pulmonary hypertension and subacute mountain sickness, which are precipitated by HA hypoxia. Any previous history of cardiopulmonary, respiratory, and infectious diseases was excluded based on their clinical examination and by administering a detailed questionnaire that also has the information about their history and background. No patients with concomitant disease were included in the study. Subjects with any of these diseases were excluded from the study. Lake Louise scoring was applied to rule out any symptoms of acute mountain sickness in the sojourners (among HAPE-f).

Blood Sample Collection. Ten milliliters of blood sample was collected from each subject in acid-citrate-dextrose anticoagulant to get plasma and cells. Blood samples of HAPE-p were drawn immediately after the diagnosis but before the start of medication. Similarly, the blood samples of the two healthy controls of the study, HAPE-f and HLs, were collected from the patient's attendants and the donors at the blood bank and staff of SNM hospital, Leh, Ladakh. Plasma was aliquoted and stored at –80 °C, whereas DNA was isolated from the blood cells and stored at –20 °C until further use.

Quantification of Apelin-13 and Nitrite Levels. Out of several peptides of apelin that activate APLNR, apelin-13 is resistant to enzymatic breakdown and is capable of retaining its biological activity for longer periods; hence, it becomes a preferred marker (1).

Plasma apelin-13 was measured by immunoassay kit (USCN Life Science) on a high-throughput SpectraMax plus384 Spectrophotometer (Molecular Devices). Absorbance was measured at 450 nm and the sample concentration was determined from the standard curve.

For nitrite levels, plasma nitrite levels were estimated by an enzymatic assay kit (Cayman Chemical). Absorbance was measured at 430 nm and the sample concentration was determined from the nitrite standard curve.

Estimation for each biomarker was performed in duplicate and the results were repeated in those samples where the coefficient of variation was >5%.

Quantitative RT-PCR Analysis of *Apelin*, *APLNR*, and *NOS3* Genes. Gene expression was performed on 10 samples each of HAPE-p, HAPE-f, and HLs. Total RNA was extracted from an aliquot of 2 mL whole blood by TRI reagent RT blood (Molecular Research Centre). RNA quantity and quality were determined on a NanoDrop ND-1000 spectrophotometer and integrity was checked by running on 1.5% agarose gel. Total RNA, 1.0 μg, was used to generate cDNA by EZ-first strand cDNA synthesis kit for RT-PCR (Biological Industries).

For real-time PCR, primers were designed by Pearl Primer software (Table S7). Real-time PCR was performed on ABI Prism 7300 Sequence Detection System (Applied Biosystems) using SYBR Green PCR Master Mix (Applied Biosystems). PCR was performed in duplicate and was repeated thrice for each gene and each sample. Relative transcript quantity was calculated using the $\Delta\Delta C_t$ method with *18SrRNA* as the endogenous reference gene.

Identification of Apelin Pathway in GWAS. A genome scan was carried out for 288 subjects (96 each of HAPE-p, HAPE-f, and HLs) using Illumina HumanOmni1-Quad BeadChips (Illumina). The bead chips were scanned on Illumina iScan system (Illumina). Genotype calls were assigned using the GenCall algorithm as implemented in Illumina Genome Studio (v2010.3; Illumina). Stringent Quality Control criteria for filtering SNPs and samples for analyses were applied separately for each group. Samples with low call rate (<95%), sex discrepancies, and cryptic relatedness (pi_hat >0.1875) were removed. SNPs with minor allele frequency <0.05 and ones that didn't follow Hardy–Weinberg equilibrium ($P < 0.0001$) were excluded. Principal component analysis was performed to assess population structure using EIGENSOFT v3.0 software. In a pathway-based approach exclusive to the apelin pathway, filtered SNPs were tested by logistic regression analysis under a log-additive model adjusting for age, sex, and the first two principal components using PLINK v1.07 software (2).

Apelin and APLNR Gene Sequencing. Of the three genes, *apelin* and *APLNR* are not studied in relation to HA. Therefore, identification of novel variants by direct sequencing of genomic DNA was performed in 30 individuals each of HAPE-p, HAPE-f, and HLs. The two genes were sequenced from 2-kb upstream of the transcription start site that covered the putative promoter region along with all of the exons and introns of the genes. Thus, the total length of 11,694 bp of *apelin* and 5,659 bp of *APLNR* was sequenced.

Selection and Genotyping of Polymorphisms. The polymorphisms of *apelin*, *APLNR*, and *NOS3* identified through GWAS and gene sequencing were selected for their validation in large sample size. All of these selected polymorphisms were also seen for functional relevance (i.e., nonsynonymous SNPs), level of heterozygosity, and position in the gene (i.e., promoter and exonic and their use in previous studies). Of several polymorphisms, 10 polymorphisms were identified in *apelin* that included 1 in the promoter, 7 in the intronic region, and 2 in the 3′ UTR; 7 polymorphisms in *APLNR* that included 3 in the promoter, 1 in the 5′ UTR, and 3 in the 3′ UTR; and 11 polymorphisms in *NOS3* that included 4 in the exonic region and 7 in the intronic region. The selected polymorphisms were genotyped in the three groups. *Apelin* and *APLNR* polymorphisms were genotyped using SNaPshot ddNTP Primer Extension PCR kit (Applied Biosystems) (Table S8), whereas *NOS3* polymorphisms were genotyped by sequenome mass spectrometry-based genotype assay using iplex gold technology (Table S9). The 4b/4a VNTR repeat of *NOS3* was analyzed by PCR amplification and the gene product bearing 4b or 4a alleles was run on 3% agarose gel to identify the allele (Table S9).

Evaluation of Functional Role of Associated SNPs. Functional role of promoter SNPs *apelin* rs3761581 and *APLNR* rs11544374 was validated by construction of reporter plasmids, transient transfection, and Luciferase activity assay. The list of primers with their cycling conditions for amplification of promoters of *apelin* and *APLNR* are provided in Table S11. Clones chosen for transfection were purified using the Qiagen plasmid mini kit (Qiagen) and were sequenced to confirm the presence of the allele. The resulting constructs were used to transiently transfect HEK-293 cells using lipofectamine 2000 reagent (Invitrogen). One microgram of construct and 20 ng of SV40-driven *Renilla* luciferase cytomegalovirus (pRL-CMV) were cotransfected to perform reporter assay. The pGL3 basic promoterless plasmid (Promega) was used as a negative control and the pGL3SV40 plasmid (Promega) as a positive control. The transfected cells were plated into 96-well plates with $\sim 6 \times 10^4$ cells per well. The cells were harvested 24 h following transfection and luciferase reporter gene activity was measured with Dual-Luciferase Reporter Assay System (Promega) in a SpectraMax 190 luminometer (Molecular Devices). Firefly luciferase activity of each allelic construct was normalized by *Renilla* luciferase pRL-CMV activity. The results were expressed as the ratio of Firefly luciferase activity divided by the pRL-CMV internal control activity and expressed as relative luciferase (mean ± SD). Three independent experiments were performed for each construct.

CpG Island of *apelin* Gene. While sequencing, one CpG island was identified only in *apelin*, which was later confirmed by the UCSC genome browser (genome.ucsc.edu/). The CpG island Searcher (cpgislands.usc.edu/) predicted the island of 1260 bp in length with 119 CpG sites spanning the 5′ UTR and portions of the promoter and intron 1. The software took into consideration the following criteria: length of island greater than 500 bp, G + C content greater than 55%, and observed CpG/expected CpG of 0.65. Methylation status was assessed in the three groups by the following sets of experiments.

Methylation Assay by Deep Sequencing.

Sodium bisulfite conversion of DNA. Bisulfite-converted DNA was prepared by EZ DNA Methylation-GoldTM Kit (Zymo Research). This method selectively converts cytosine (C) to uracil (U) without significant transformation of 5-methylcytosine (5mC) to thymine (T). The bisulfite-converted DNA was PCR-amplified using the bisulfite-conversion–based methylation PCR primers designed by the software methprimer (www.urogene.org/cgi-bin/methprimer/methprimer.cgi) (Table S12). Detection of U vs. 5mC was accomplished by sequencing the bisulfite converted PCR amplicons through Ion Torrent Personal Genome Machine (PGM) (Life Technologies). The length and concentration of these amplicons were analyzed using Agilent High Sensitivity DNA chip on Agilent 2100 bioanalyzer (Agilent Technologies).

Amplicon library generation and emulsion PCR. Amplicon library was prepared by the Ion Plus Fragment Library Kit (Life Technologies). The quality and quantity of the libraries were quantified by High Sensitivity DNA kit on Agilent 2100 Bioanalyzer (Agilent Technologies). These libraries were sequenced using 316 PGM and Ion Sequencing Kit v2.0 (Life Technologies).

CpG island sequence analysis. Signal processing and base calling was performed on Galaxy platform (https://usegalaxy.org/). The FASTAQ files obtained from PGM were transformed to FASTA files to analyze for Phred quality control. The qualified FASTA files were aligned with the reference genome using DNAstar MegAlign sequence analysis tool (DNAstar, windows 32 protean 5.07.1989–2003; DNAstar) and the percentage of Cs and Ts was determined among all reads aligned to each C in genomic DNA sequence.

Statistical Analyses. Genotype and allele distributions, OR, and 95% confidence interval (CI) were calculated by multivariate-logistic regression using SPSS-15.0; the covariates were age, sex, and BMI. Hardy–Weinberg equilibrium was checked using the χ^2 goodness-of-fit test. Permutation analysis for haplotype evaluation was performed by the algorithm developed by Stephens et al. (Phase-2.1) (3). The polymorphisms were checked for tagging efficiency with a cut-off r^2 of ≥ 0.8 using the software Tagger (Haploview-4.0, www.broadinstitute.org/scientific-community/science/programs/medical-and-population-genetics/haploview/haploview). The interactions of

genotypes were evaluated by multidimensional reduction-v1.2.2 (MDR-1.2.2) (4). The quantitative RT-PCR data were analyzed by one-way analysis of variance. The Pearson's correlation (r) evaluated the correlation between the two continuous variables. The association of major genotypes and haplotypes with relevant bio-levels was performed using binary-logistic regression analysis. The unpaired Student's t test was used for the comparisons between the groups. Values are represented as mean ± SD. A P value < 0.05, after adjustment with confounders and Bonferroni's multiple correction was considered statistically significant.

1. Ashley EA, et al. (2005) The endogenous peptide apelin potently improves cardiac contractility and reduces cardiac loading in vivo. *Cardiovasc Res* 65(1):73–82.
2. Purcell S, et al. (2007) PLINK: A tool set for whole-genome association and population-based linkage analyses. *Am J Hum Genet* 81(3):559–575.
3. Stephens M, Smith NJ, Donnelly P (2001) A new statistical method for haplotype reconstruction from population data. *Am J Hum Genet* 68(4):978–989.
4. Hahn LW, Ritchie MD, Moore JH (2003) Multifactor dimensionality reduction software for detecting gene-gene and gene-environment interactions. *Bioinformatics* 19(3):376–382.

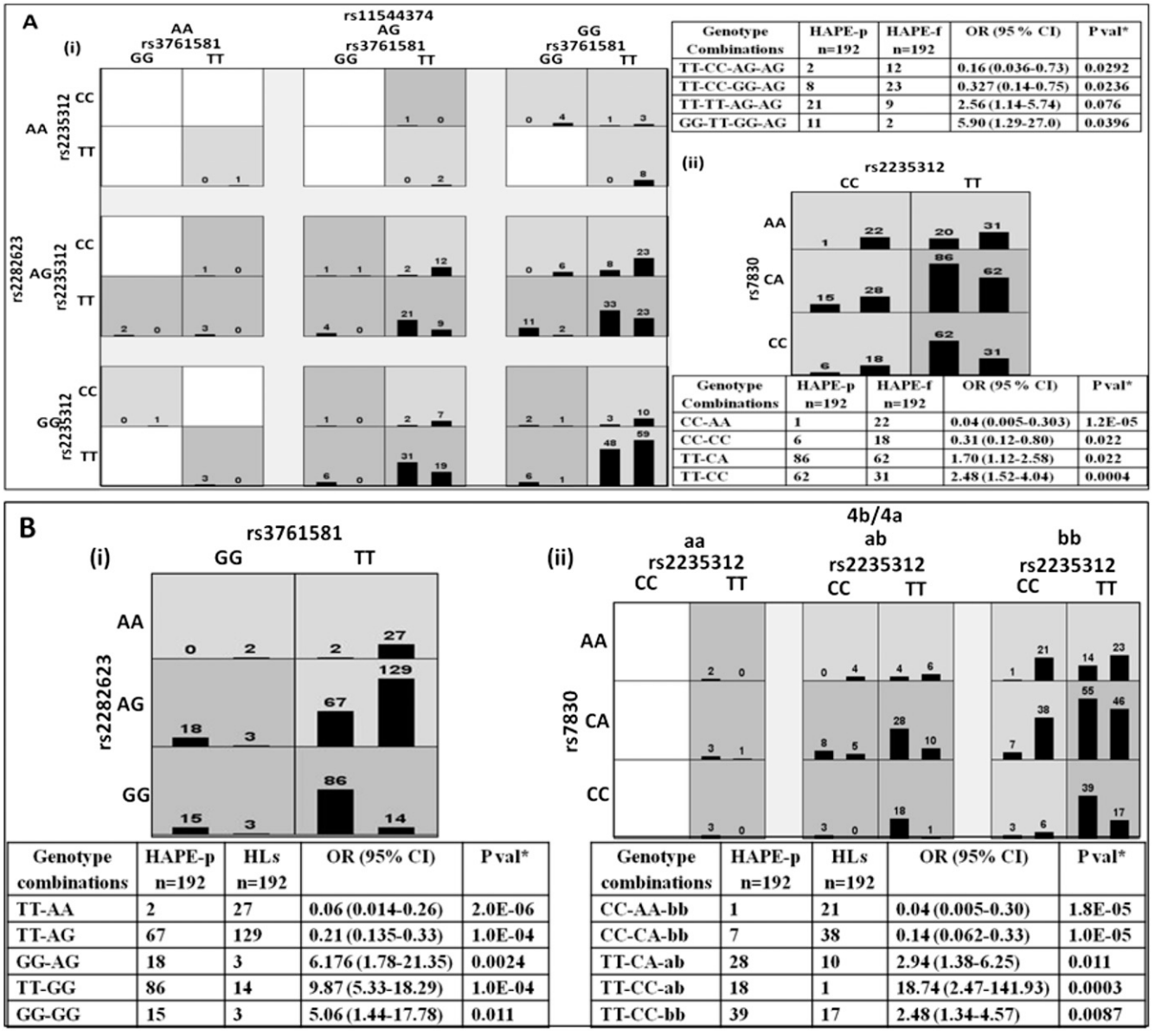

Genotype Combinations	HAPE-p n=192	HAPE-f n=192	OR (95 % CI)	P val*
TT-CC-AG-AG	2	12	0.16 (0.036-0.73)	0.0292
TT-CC-GG-AG	8	23	0.327 (0.14-0.75)	0.0236
TT-TT-AG-AG	21	9	2.56 (1.14-5.74)	0.076
GG-TT-GG-AG	11	2	5.90 (1.29-27.0)	0.0396

Genotype Combinations	HAPE-p n=192	HAPE-f n=192	OR (95 % CI)	P val*
CC-AA	1	22	0.04 (0.005-0.303)	1.2E-05
CC-CC	6	18	0.31 (0.12-0.80)	0.022
TT-CA	86	62	1.70 (1.12-2.58)	0.022
TT-CC	62	31	2.48 (1.52-4.04)	0.0004

Genotype combinations	HAPE-p n=192	HLs n=192	OR (95% CI)	P val*
TT-AA	2	27	0.06 (0.014-0.26)	2.0E-06
TT-AG	67	129	0.21 (0.135-0.33)	1.0E-04
GG-AG	18	3	6.176 (1.78-21.35)	0.0024
TT-GG	86	14	9.87 (5.33-18.29)	1.0E-04
GG-GG	15	3	5.06 (1.44-17.78)	0.011

Genotype combinations	HAPE-p n=192	HLs n=192	OR (95% CI)	P val*
CC-AA-bb	1	21	0.04 (0.005-0.30)	1.8E-05
CC-CA-bb	7	38	0.14 (0.062-0.33)	1.0E-05
TT-CA-ab	28	10	2.94 (1.38-6.25)	0.011
TT-CC-ab	18	1	18.74 (2.47-141.93)	0.0003
TT-CC-bb	39	17	2.48 (1.34-4.57)	0.0087

Fig. S1. Multidimensional reduction results depicting interactions between apelin, APLNR, and NOS3. (*A*) Distribution of interactions between: (*i*) *Apelin* and *APLNR* in a four-locus rs3761581, rs2235312, rs11544374, and rs2282623 model and (*ii*) *Apelin* and *NOS3* in a two-locus rs2235312 and rs7830 were selected as best MDR models in HAPE-p and HAPE-f. (*B*) Distribution of interactions between (*i*) *Apelin* and *APLNR* in a two-locus, rs3761581 and rs2282623 model and (*ii*) *Apelin* and *NOS3* in a three-locus rs2235312, rs7830, and 4b/4a were selected as best MDR models in HAPE-p and HLs. Boxes with dark shade depict high risk, boxes with light shade depict low risk, and boxes with no shade/white depict blank; the latter represents no combination.

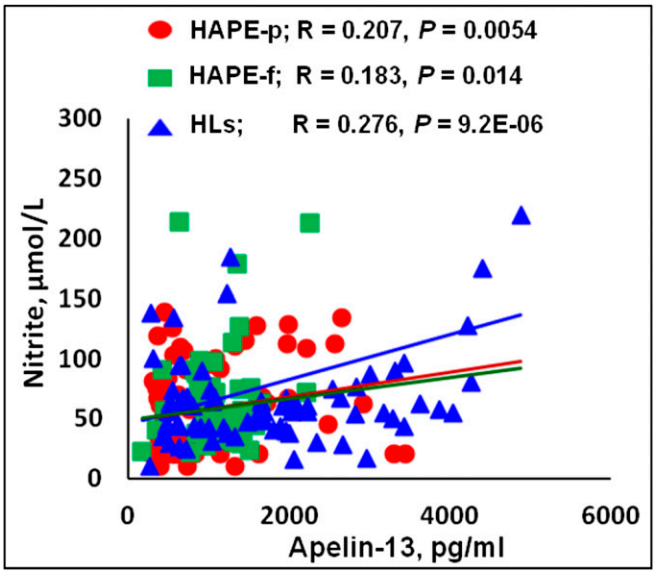

Fig. S2. Correlation between apelin-13 and nitrite levels. A significant positive correlation was found between the two levels in HAPE-p, HAPE-f, and HLs (P = 0.005, 0.014, and 9.2E-06, respectively).

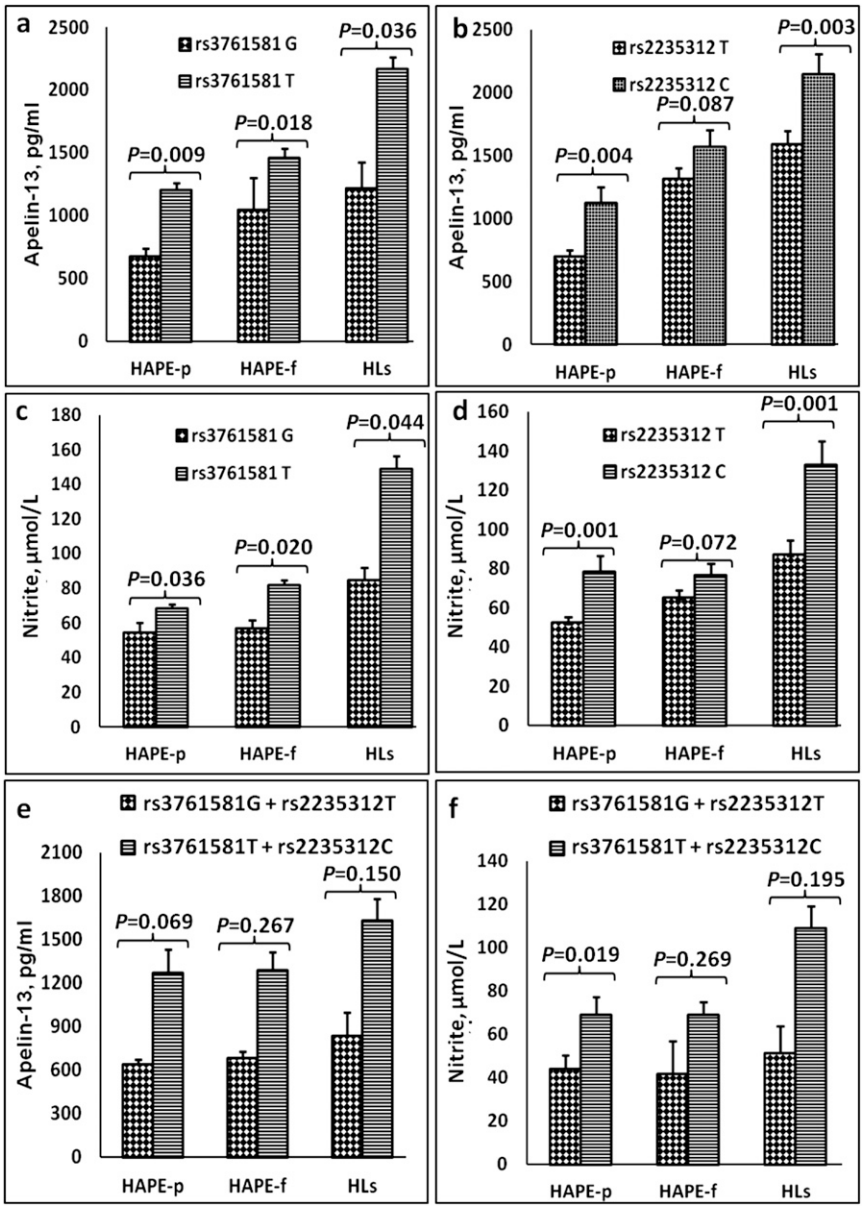

Fig. S3. Association of plasma levels of apelin-13 and nitrite with alleles of rs3761581 and rs2235312 in HAPE-p, HAPE-f, and HLs. Contribution of individual alleles of polymorphisms (*A*) rs3761581 and (*B*) rs2235312 to apelin-13 levels. Contribution of individual alleles of polymorphisms (*C*) rs3761581 and (*D*) rs2235312 to nitrite levels. Contribution of the combined alleles rs3761581T + rs2235312C to the levels of (*E*) apelin-13 and (*F*) nitrite. The results are presented as mean ± SE.

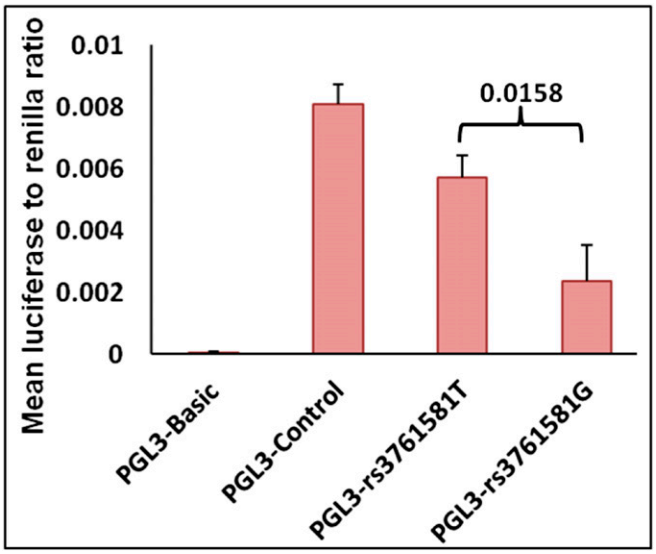

Fig. S4. Effect of the SNP rs3761581 on the transcriptional activity of apelin promoter. The pGL3 vector with rs3761581G allele produced a 58.6% decrease in the relative luciferase activity compared with that of rs3761581T allele in vitro ($P = 0.016$). Luciferase activity was normalized to control plasmid (pRL-CMV) expression. The results are shown as the mean ± SE ($n = 3$). The apelin promoter vectors pGL3-rs3761581T (major allele) and pGL3-rs3761581G (minor allele) were transfected into HEK-293 cells. pGL3-Basic and pGL3-SV40 were used as negative and positive control vectors, respectively. Relative luciferase activity was measured 24 h posttransfection. Data are expressed as the mean luciferase to *Renilla* ratios. A one-way ANOVA was used to assess statistical significance between the two vectors.

Table S1. Clinical characteristics of the HAPE-p, HAPE-f, and HLs

				P values		
Clinical characteristics	HAPE-p (*n*)	HAPE-f (*n*)	HLs (*n*)	HAPE-p vs. HAPE-f	HAPE-p vs. HLs	HAPE-f vs. HLs
Age, y	29.1 ± 13.86 (200)	27.8 ± 10.4 (200)	39.05 ± 7.44 (200)	0.263	<0.0001	<0.0001
SBP, mmHg	124.6 ± 21.1 (200)	119.8 ± 3.5 (200)	121 ± 8.0 (200)	0.001	0.001	0.04
DBP, mmHg	82.7 ± 17.0 (200)	80.4 ± 10.0 (200)	81.1 ± 10.0 (200)	0.085	0.122	0.406
MAP, mmHg	96.7 ± 16.0 (200)	93.5 ± 10.0 (200)	94.4 ± 10.0 (200)	0.012	0.021	0.285
PR, rate/min	92.2 ± 22.9 (200)	80.1 ± 19.9 (200)	84.0 ± 15.7 (200)	<0.0001	<0.0001	0.007
SaO_2 levels, %	71.7 ± 12.5 (200)	91.2 ± 3.7 (200)	89.6 ± 3.2 (200)	<0.0001	<0.0001	<0.0001
PASP, mmHg	50.1 ± 9.00 (90)	29.2 ± 3.77 (35)	30.33 ± 6.31 (55)	<0.0001	<0.0001	0.34

Data are presented as mean ± SD and are compared by unpaired Student's *t* test. DBP, diastolic blood pressure; MAP, mean arterial pressure; *n*, number of subjects; PASP, pulmonary artery systolic pressure PR, pulse rate; SaO_2, arterial oxygen saturation; SBP, systolic blood pressure.

Table S2. An apelin pathway based selection of SNPs from the data of GWAS of the three studied groups

Genes	SNPs
AGT	rs7536290, rs10864770, rs2067853, rs7079, rs5044, rs2478523, rs2478522, rs2493132, rs3789671, rs2478545, rs6687360, rs699, rs4762, rs11122576, rs2004776, rs3889728, rs2493134, rs3789679, **rs2148582**, rs5051, rs5050, rs11568020
AGTR1	rs275650, rs275651, rs1492078, rs2131127, rs931490, rs4681443, rs4681444, rs1492098, rs3772616, rs4524238, rs12695891, rs12721242, rs12695894, rs12695902, rs12695904, rs3772614, rs6801836, rs1800766, rs418061, rs12695923, rs5183, rs5186, rs5187, rs35533650, rs380400
AMPK	rs7708957, rs6870698, rs6882903, rs1002424, rs1002423, rs17239241, rs257009, rs11745121, rs11747210, rs12188129, rs11749437, rs10053664, rs11749772, rs3805486
NOS3	rs34204527, rs11771443, rs3918226, kgp13507464, rs35281220, rs41508746, rs2853792, rs3918227, rs3918228, **rs3918184**, rs3918185, **rs3918186**, rs3918187, rs2566511, rs3918229, rs2853795, rs2566513, rs2853796, **rs3730305**, **rs891511**, rs3918230, rs3918196, rs3918231, rs753482, rs3918232, **rs743506**, rs3730009, rs3918201, **rs743507**, kgp22847056, rs3918233, rs867225, rs3918234, rs6947833, rs891512, **rs1808593**, rs3918235, rs3918236, kgp22844809, **rs7830**, rs3918208, rs3918211
KLF4	rs10816519, rs11793219, rs11794295
APLNR	rs2282623, rs2282624, rs746886, rs948846, rs746887, rs12270028, rs7943508, rs948847
KLF2	**rs10424657**, rs7248864, **rs12462380**, rs1003669, rs15336, rs11086029
ACE2	**rs1514283**, rs2074192, rs4646180, rs4646179, rs1514280, rs4240157, rs4646140, rs2048683, rs2285666, rs4646134, rs4646113
Apelin	rs12559440, rs3131266, rs12861986, rs3115759, rs3115758, rs909657, **rs2235312**

A total of 138 SNPs from nine different genes of apelin pathway were identified in the data. SNPs marked in bold were found to be significantly associated with adaptation and mal-adaptation of HA. *ACE2*, *angiotensin converting enzyme 2*; *AGT*, *angiotensinogen*; *AMPK*, *α 1 catalytic subunit*; *KLF2 and -4*, *Kruppel-like factor 2 and 4.*

Table S3. Allele frequency of the polymorphisms rs3761581, rs2235312, and rs3115757 of *apelin* in HAPE-p, HAPE-f, and HLs

	HAPE-f	HAPE-p	HLs	HAPE-f vs. HAPE-p		HAPE-p vs. HLs		HLs vs. HAPE-f	
Polymorphism/allele	Distribution (%)			OR (95% CI)	*P* value	OR (95% CI)	*P* value	OR (95% CI)	*P* value
rs3761581									
T	184 (92)	147 (82)	170 (92)	1		1		1	
G	16 (8)	33 (18)	8 (3)	2.58 (1.37–4.87)	0.0027	4.77 (2.14–10.65)	3.9E-05	0.54 (0.23–1.29)	0.16
rs2235312									
C	68 (34)	22 (12)	74 (26.5)	1		1		1	
T	132 (66)	158 (88)	108 (55.5)	3.70 (2.17–6.31)	1.0E-06	5.11 (2.99–8.74)	1.2E-06	0.72 (0.48–1.10)	0.13
rs3115757									
C	36 (18)	14 (8)	26 (10.5)	1		1		1	
G	164 (82)	166 (92)	152 (68.5)	2.60 (1.35–5.00)	0.0032	2.03 (1.02–4.03)	0.04	1.28 (0.74–2.23)	0.37

P values were obtained after adjustment with age, sex, and BMI by multivariate-logistic regression analysis using SPSS 15.0 software. The allele frequency was compared by χ^2 test. *n*, number; %, percent distribution.

Table S4. Genotype and allele distribution of the polymorphisms rs11544374 and rs2282623 of *APLNR* in HAPE-p, HAPE-f, and HLs

	HAPE-f	HAPE-p	HLs	HAPE-f vs. HAPE-p		HAPE-p vs. HLs		HLs vs. HAPE-f	
Polymorphisms and genotype/allele	Distribution (%)			OR (95% CI)	*P* value	OR (95% CI)	*P* value	OR (95% CI)	*P* value
rs11544374									
GG	148 (74)	112 (62)	136 (68)	1		1		1	
GA	50 (25)	59 (33)	60 (30)	1.60 (1.00–2.40)	0.05	1.19 (0.77–1.85)	0.43	1.29 (0.84–2.04)	0.23
AA	2 (1)	9 (5)	4 (2)	5.95 (1.30–28.1)	0.011	2.73 (0.82–9.11)	0.09	2.17 (0.39–12.0)	0.36
G	346 (87)	283 (76)	332 (83)	1		1		1	
A	54 (13)	77 (24)	68 (17)	1.74 (1.20–2.50)	0.004	1.33 (0.92–1.91)	0.12	1.31 (0.89–1.92)	0.17
rs2282623									
AA	20 (10)	2 (1)	36 (18)	1		1		1	
AG	78 (39)	74 (41)	120 (60)	9.48 (2.14–42.0)	4.6E-04	11.1 (2.59–47.5)	7.8E-05	0.85 (0.46–1.58)	0.62
GG	102 (51)	104 (58)	44 (22)	10.2 (2.32–44.7)	2.0E-04	42.5 (9.81–184)	1.2E-10	0.24 (0.12–0.46)	9.0E-06
A	118 (29.5)	78 (22)	192 (48)	1		1		1	
G	282 (70.5)	282 (78)	208 (52)	1.50 (1.08–2.10)	0.013	0.30 (0.22–0.41)	1.0E-07	0.45 (0.34–0.61)	4.5E-05

P values were obtained after adjustment with age, sex, and BMI by multivariate-logistic regression analysis using SPSS 15.0 software. The genotype distribution and allele frequency were compared by χ^2 test. *n*, number; %, percent distribution.

Table S5. Genotype and allele distribution of the polymorphisms 4b/4a, rs1799983, and rs7830 of *NOS3* in HAPE-p, HAPE-f, and HLs

Polymorphisms and genotype/allele	HAPE-f	HAPE-p	HLs	HAPE-f vs. HAPE-p		HAPE-p vs. HLs		HLs vs. HAPE-f	
	Distribution (%)			OR (95% CI)	*P* value	OR (95% CI)	*P* value	OR (95% CI)	*P* value
4b/4a									
bb	154 (77)	110 (61)	170 (85)	1		1		1	
vba	44 (22)	62 (34)	28 (14)	1.97 (1.25–3.12)	0.003	3.42 (2.06–5.68)	1.0E-06	1.73 (1.03–2.92)	0.04
aa	2 (1)	8 (4)	2 (1)	5.6 (1.17–26.9)	0.016	6.18 (1.29–29.6)	0.01	0.91 (0.13–6.51)	1
b	352 (88)	282 (78)	368 (92)	1		1		1	
a	48 (12)	78 (22)	32 (8)	2.03 (1.37–3.00)	0.0003	3.18 (2.05–4.94)	9.0E-07	0.64 (0.39–1.02)	0.06
rs1799983									
GG	137 (68.5)	115 (64)	158 (79)	1		1		1	
GT	54 (27)	43 (24)	36 (18)	0.95 (0.59–1.52)	0.826	1.64 (1.0–2.72)	0.053	0.58 (0.36–0.93)	0.02
TT	9 (4.5)	22 (12)	6 (3)	2.91 (1.29–6.57)	0.0077	5.04 (1.98–12.8)	0.00023	0.58 (0.20–1.66)	0.30
G	328 (82)	273 (76)	352 (88)	1		1		1	
T	72 (18)	87 (24)	48 (12)	1.45 (1.02–2.06)	0.037	2.34 (1.59–3.44)	1.2E-05	0.62 (0.42–0.92)	0.02
rs7830									
AA	54 (27)	21 (11.7)	54 (27)	1		1		1	
AC	101 (50.5)	90 (50)	106 (53)	2.3 (1.28–4.08)	0.0044	2.18 (1.23–3.89)	0.0073	1.05 (0.66–1.67)	0.84
CC	45 (22.5)	69 (38)	40 (20)	3.94 (2.1–7.39)	1.2E-05	4.43 (2.34–8.38)	3.0E-06	0.89 (0.50–1.57)	0.68
A	209 (52.25)	132 (37)	214 (53.5)	1		1		1	
C	191 (47.75)	228 (63)	186 (46.5)	1.89 (1.41–2.53)	1.6E-05	1.98 (1.48–2.66)	3.0E-06	0.95 (0.72–1.25)	0.72

P values were obtained after adjustment with age, sex, and BMI by multivariate-logistic regression analysis using SPSS 15.0 software. The genotype distribution and allele frequency were compared by χ^2 test. *n*, number; (%), percent distribution.

Table S6. Distribution of significant haplotypes of the polymorphisms rs3761581, rs2235312, and rs3115757 of *apelin*; rs11544374 and rs2282623 of *APLNR*; and 4b/4a, rs1799983, and rs7830 of *NOS3* in HAPE-p, HAPE-f, and HLs

Genes/haplotypes	HAPE-f	HAPE-p	HLs	HAPE-p vs. HAPE-f		HAPE-p vs. HLs		HLs vs. HAPE-f	
	Distribution (%)			OR (95% CI)	*P*	OR (95% CI)	*P*	OR (95% CI)	*P*
Apelin									
G-T-G	1.0	14.5	2.0	16.22 (5.82–45.21)	1.0E-06	7.42 (3.61–15.2)	1.0E-06	2.19 (0.67–7.16)	0.55
T-T-G	59.0	68.0	51.0	1.50 (1.12–2.02)	0.021	2.04 (1.53–2.73)	3.0E-06	1.36 (1.03–1.80)	0.10
T-C-C	10.0	1.0	8.0	0.09 (0.03–0.26)	1.0E-06	0.12 (0.04–0.34)	9.0E-06	0.75 (0.46–1.22)	0.72
T-C-G	18.0	8.0	24.0	0.41 (0.26–0.64)	1.6E-04	0.28 (0.18–0.44)	1.0E-06	1.44 (1.02–2.03)	0.12
APLNR									
A-A	1.0	1.5	3.0	2.01 (0.50–8.12)	0.31	0.54 (0.19–1.47)	0.22	3.74 (1.04–13.5)	0.06
A-G	12.5	21.0	14.0	1.87 (1.26–2.76)	0.0028	1.63 (1.12–2.34)	0.02	1.14 (0.75–1.74)	0.52
G-A	28.5	21.0	49.0	0.66 (0.48–0.92)	0.03	0.27 (0.20–0.38)	0.001	2.42 (1.79–3.26)	0.001
G-G	58.0	56.5	34.0	0.93 (0.69–1.23)	0.61	2.51 (1.87–3.36)	0.001	0.37 (0.27–0.49)	0.001
NOS3									
b-G-A	40.3	30	49.8	0.69(0.53–0.91)	0.022	0.43 (0.3–0.57)	<0.0001	1.46 (1.1–1.9)	0.012
b-T-A	6.0	2.0	3.0	0.34(0.15–0.77)	0.019	0.7 (0.3–1.6)	0.41	0.5 (0.2–0.9)	0.066
a-G-C	7.3	14.0	7.9	1.97(1.22–3.13)	0.013	1.4 (1.15–1.7)	0.0075	1.1 (0.7–1.8)	0.74
a-T-C	0	1.3	3.5	—	0.018	0.37 (0.14–1.0)	0.12	—	0.0024

P values were obtained by multivariate-logistic regression analysis and Bonferroni's multiple correction test ($P < 0.05$) after adjustment with age, sex, and BMI using SPSS 15.0 software. %, percent distribution.

Table S7. Real-time PCR conditions for *apelin, APLNR, NOS3*, and *18srRNA*

Gene	Primer sequence	Cycling conditions	Product size (bp)
Apelin	F 5′-GCG GTT ATG TCT CCT CCA TAG ATT-3′ R 5′-GTG CGA GGT GAG AGC TGA ATG-3′	I94 °C 10′, D94 °C 15″, A60 °C 60″, 40 cy	70
APLNR	F 5′-CTA TCC TGT TTT CTG AGT GTG AGG-3′ R 5′-CTA AGG GCT GGA GCA CTA ATT ATC-3′	I94 °C 10′, D94 °C 15″, A60 °C 60″, 40 cy	170
NOS3	F 5′- TCT ATG GAT GAG TAT GAC GTG G-3′ R 5′-CGG ATC TTA TAA CTC TTG TGC TG-3′	I94 °C 10′, D94 °C 15″, A60 °C 60″, 40 cy	150
18srRNA	F 5′-GTA ACC CGT TGA ACC CCA TT-3′ R 5′-CCA TCC AAT CGG TAG TAG CG-3′	I94 °C 10′, D94 °C 15″, A60 °C 60″, 40 cy	155

A, annealing; cy, cycles; D, denaturation; F, forward; I, initial denaturation; R, reverse.

Table S8. Primers and PCR conditions of the polymorphisms of *apelin* and *APLNR*

SNP and rs ID	Primer sequence	Cycling conditions	Product size (bp)
Apelin			
rs3761581	F 5′-AGA TCC AGA AGA GTG AGA AGA C -3′ R 5′-CAG GAT AAC ACT AAT CCA GCA G-3′ IP 5′-TCC AGG GAA CAA GAA AGG G-3′	I95 °C 5′, D95 °C 30″, A58.8 °C 30″, E72 °C 45″, 35cy, FE72 °C 10′	347
rs2281068	F 5′-AGA CTT GGT TCT CTT ACA TCC T-3′ R 5′-GAG ACA TTG ACA CAG AGG AC-3′ IP 5′-CTT TCT GTC CCA GGC ACG G-3′	I95 °C 5′, D95 °C 30″, A64 °C 30″, E72 °C 45″, 35cy, FE72 °C 10′	263
rs2235312	F 5′-CTC TAT TCA AGA CCT GAA CAC G-3′ R 5′-GTC TGA GTG GTT GTC TAT TGG-3′ IP 5′-CAC CAC AGT AAG AAG TGG G-3′	I95 °C 5′, D95 °C 30″, A66.2 °C 30″, E72 °C 45″, 35cy, FE72 °C 10′	370
rs2235310	F 5′-TCT CAC TGA CTT CTC TAC TCC-3′ R 5′-TTC TCA GAC TCA CAA GAG CA-3′ IP 5′-GAG GCA GCG TGG AGA GGG G-3′	I95 °C 5′, D95 °C 30″, A58.8 °C 30″, E72 °C 45″, 35cy, FE72 °C 10′	363
rs2235308	F 5v-GTG ATG CTG AGG ACA ATG AG-3′ R 5′-GAA AGA CCT TCA CTA AGC TCC-3′ IP 5′-GGG AGG GAT GCA AGA AGC C-3′	I95 °C 5′, D95 °C 30″, A63.4 °C 30″, E72 °C 45″, 35cy, FE72 °C 10′	523
rs2235307	F 5′-GTG ATG CTG AGG ACA ATG AG-3′ R 5′-GAA AGA CCT TCA CTA AGC TCC-3′ IP 5′-ATC AGC ATC ATT CAG ATC C-3′	I95 °C 5′, D95 °C 30″, A63.4 °C 30″, E72 °C 45″, 35cy, FE72 °C 10′	523
rs909657	F 5′-AGG AAT TTA CAT GAG ACA CAG G-3′ R 5′-AAC ATC ACG TCA TTG TAC TCC-3′ IP 5′-TGC TGA AGG TGA CCA TTG T-3′	I95 °C 5′, D95 °C 30″, A65 °C 30″, E72 °C 45″, 35cy, FE72 °C 10′	406
rs3115757	F 5′-ACA CAT CCA TCA AAC AGT CC-3′ R 5′-TTC TTC CCT CCT TCT CAC AG-3′ IP 5′-CTA GCC CCT TTA TTT TAC A-3′	I95 °C 5′, D95 °C 30″, A62 °C 30″, E72 °C 45″, 35cy, FE72 °C 10′	377
rs3115758	F 5′-TTC CTT TGG CCT AGG ATA TGT C-3′ R 5′-TTC TCT GCA TTC TTC CCT GG-3′ IP 5′-CCC CCA AGT GCC CAC CCC C-3′	I95 °C 5′, D95 °C 30″, A63.2 °C 30″, E72 °C 45″, 35cy, FE72 °C 10′	519
rs3115759	F 5′-TTC CTT TGG CCT AGG ATA TGT C-3′ R 5′-TTC TCT GCA TTC TTC CCT GG-3′ IP 5′-CCT GAG CGC GGG GTG GAA-3′	I95 °C 5′, D95 °C 30″, A63.2 °C 30″, E72 °C 45″, 35cy, FE72 °C 10′	519
APLNR			
rs7119375	F 5′-CTT CAA GGT TGT GGA AAG GG-3′ R 5′-GTG AAT GGC TGT TGA GTG AG-3′ IP 5′-CGT AGT AAT TCT TAC ACT-3′	I95 °C 5′, D95 °C 30″, A65 °C 30″, E72 °C 45″, 35cy, FE72 °C 10′	289
rs10501367	F 5′-TAA TTT CAG CAC TTT GGG AGG-3′ R 5′-CTT TAG AAG GTT GAG GGC AG-3′ IP 5′-CGA CAT GCC AGG TAC TGT-3′	I95 °C 5′, D95 °C 30″, A64.7 °C 30″, E72 °C 45″, 35cy, FE72 °C 10′	452
rs9943582	F 5′-GGT AGA GAA AGA TGA AGC GAG-3′ R 5′-GGG CTG AAC ATT ATC TGT GG-3′ IP 5′-TCC CAT TTA GAT TGG ATG G-3′	I95 °C 5′, D95 °C 30″, A61 °C 30″, E72 °C 45″, 35cy, FE72 °C 10′	416
rs11544374	F 5′-TGC AAG GAA GTG TCT TAA CTG-3′ R 5′-GGA TTT CCA GTC TGT GTA CTC-3′ IP 5′-AGC CCT TCT TAC TCT CTG A-3′	I95 °C 5′, D95 °C 30″, A59.3 °C 30″, E72 °C 45″, 35cy, FE72 °C 10′	334
rs746886	F 5′-GTC ATT TGG ACA AAC CTC CT-3′ R 5′-TTA ATT TCA TCC TCA CGG TCT C-3′ IP 5′-ACT GCA ACT CTG CTG TTC A-3′	I95 °C 5′, D95 °C 30″, A60 °C 30″, E72 °C 45″, 35cy, FE72 °C 10′	596
rs2282624	F 5′-GTC ATT TGG ACA AAC CTC CT-3′ R 5′-TTA ATT TCA TCC TCA CGG TCT C-3′ IP 5′-GCC AAG GCT TGG GGG C-3′	I95 °C 5′, D95 °C 30″, A60 °C 30″, E72 °C 45″, 35cy, FE72 °C 10′	596
rs2282623	F 5′-GTC ATT TGG ACA AAC CTC CT-3′ R 5′-TTA ATT TCA TCC TCA CGG TCT C-3′ IP 5′-CCT CCC TTG GCC CCT TTC C-3′	I95 °C 5′, D95 °C 30″, A60 °C 30″, E72 °C 45″, 35cy, FE72 °C 10′	596

A, annealing; cy, cycles; D, denaturation; E, extension; F, forward; FE, final extension; I, initial denaturation; IP, internal primer; R, reverse.

Table S9. Sequence of the preamplification PCR primers (PCRP) and iPLEX primers designed for multiplex genotyping of 10 polymorphisms of *NOS3* by the iPLEX assays of Sequenom MassARRAY system

S.No.	rs ID	Second PCRP sequence	First PCRP sequence	iPLEX primer
1	rs1800779	ACGTTGGATGAGCTAGTGGCCTTTCTCCAG	ACGTTGGATGAGCACTCTCCAGGCACTTCA	tGCCTTTCTCCAGCCCCTCAGATG
2	rs1541861	ACGTTGGATGGCTCCAGGCTTTAATTTCTC	ACGTTGGATGCCCATAGCTCTAGAGCTTTC	gCTCTAAAATGGGTCTTAACCTTT
3	rs1799983	ACGTTGGATGAAACGGTCGCTTCGACGTG	ACGTTGGATGGGGCAGAAGGAAGAGTTC	ggCCTGCTGCTGCAGGCCCCAGATGA
4	rs1800780	ACGTTGGATGTCCCAAAACCCTGTTGTGAG	ACGTTGGATGTGCGGGAGAGGAAGGTGTGA	aCCCTGCCTCTGTGCACCC
5	rs7830	ACGTTGGATGCTGTCCCTAGATTGTGTGAC	ACGTTGGATGCGGCTGCATGACATTGAGAG	gaTTCAGGCAGTCCTTTAGTC
6	rs1549758	ACGTTGGATGACTTCCGAATCTGGAACAGC	ACGTTGGATGGTGATCTCCACGTTGGCTG	gtGCGGGCTACCGGCAGCAGGA
7	rs3918211	ACGTTGGATGGGGCCACATGTTTGTCTGC	ACGTTGGATGTGCACGGTCTGCAGGACGTT	GTTTGTCTGCGGCGATGT
8	rs3918227	ACGTTGGATGTTCATAATAGCCCCGACCTG	ACGTTGGATGTGAGTGCCGTTCATTGTGTG	gaaaAAGTGTCACCAACAAGAGAATG
9	rs1800783	ACGTTGGATGATCTTCTACCATGCTGGAGG	ACGTTGGATGAGTCATCCTTGGTCATGCAC	gATGCTGGAGGAGACAACAGA
10	rs2070744	ACGTTGGATGACCAGGGCATCAAGCTCTTC	ACGTTGGATGATTCAGTGACGCACGCTTCC	CATCAAGCTCTTCCCTGGC

Table S10. PCR conditions of 4b/4a repeat polymorphism of *NOS3*

SNP	rs ID	Primer sequence	Cycling conditions	Product size (bp)
NOS3	4b/4a	F 5′– AGG CCC TAT GGT AGT GCC TTT –3′ R 5′– TCT CTT AGT GCT GTG GTC AC –3′	I94 °C 4′, D94 °C 30″, A65 °C 30″, E72 °C 45″, 30cy, FE72 °C 10′	bb = 420 aa = 393

A, annealing; cy, cycles; D, denaturation; F, forward; I, initial denatureation; R, reverse.

Table S11. Primers and cycling conditions for amplification of promoter polymorphisms rs3761581 and rs11544374 of *apelin* and *APLNR*, respectively

Gene	Primer sequence	Cycling conditions
Apelin	F 5′– GTT GTT CTC GAG AGA TCC AGA AGA GTG AGA AGA C–3′ R 5′– GTT GTT AAG CTT CAG GAT AAC ACT AAT CCA GCA G–3′	I94 °C 5′, D94 °C 45″, A65 °C 30″, E72 °C 45″, 30cy, FE72 °C 10′
APLNR	F 5′– GTT GTT CTC GAG AAT GTA TCC ATG TTC TCA CC–3′ R 5′– GTT GTT AAG CTT GAT TTC CAG TCT GTG TAC TC–3′	I94 °C 5′, D94 °C 1.5′, A65 °C 30″, E72 °C 1.5′, 35cy, FE72 °C 10′

A, annealing; cy, cycles; D, denaturation; F, forward; I, initial denaturation; R, reverse.

Table S12. Bisulfite-conversion–based methylation PCR primers and their cycling conditions

Gene	Primer sequence	Cycling conditions	Product size (bp)
MET_AP1	F 5′–GGA GTG GTT GTA GGT TGT TAG AGA G–3′ R 5′–ACT TAA CCA CAA ACC CAC TTA ATC A–3′	I94 °C 4′, D94 °C 30″, A60 °C 30″, E72 °C 30″, 35cy, FE72 °C 7′	204
MET_AP2	F 5′–GAG TGG TTG TAG GTT GTT AGA G–3′ R 5′–ACT TAA CCA CAA ACC CAC TTA ATC–3′	I94 °C 4′, D94 °C 30″, A60 °C 30″, E72 °C 30″, 35cy, FE72 °C 7	204
MET_AP3	F 5′–TGT GTA TAT TTA GTG GTT GGG GAG T–3′ R 5′–AAC AAA AAC ACC TAC ACA CAA AAC C–3′	I94 °C 4′, D94 °C 30″, A60 °C 30″, E72 °C 30″, 35cy, FE72 °C 7	177
MET_AP4	F 5′–GTG TAT ATT TAG TGG TTG GGG AG–3′ R 5′–AAC AAA AAC ACC TAC ACA CAA AAC C–3′	I94 °C 4′, D94 °C 30″, A60 °C 30″, E72 °C 30″, 35cy, FE72 °C 7	177
MET_AP5	F 5′–TTT TTG GAG TTG TTG AGG TTA GTT T–3′ R 5′–TCC CCA ACC ACT AAA TAT ACA CAC T–3′	I94 °C 4′, D94 °C 30″, A60 °C 30″, E72 °C 30″, 35cy, FE72 °C 7	121
MET_AP6	F 5′–TTT TTG GAG TTG TTG AGG TTA GTT T–3′ R 5′–CCC AAC CAC TAA ATA TAC ACA CT–3′	I94 °C 4′, D94 °C 30″, A60 °C 30″, E72 °C 30″, 35cy, FE72 °C 7	121
MET_AP7	F 5′–TTG TGG TGT GTG GAG GTG AG–3′ R 5′–ATA ACT CAA AAC ACT CTA TCA ATC TAC–3′	I94 °C 4′, D94 °C 30″, A60 °C 30″, E72 °C 30″, 35cy, FE72 °C 7	180

A, annealing; cy, cycles; D, denaturation; E, extension; F, forward; FE, final extension; I, initial denaturation; R, reverse.